Pattern formation in a reaction-diffusion system of Fitzhugh-Nagumo type before the onset of subcritical Turing bifurcation

Maxim Kuznetsov,* Andrey Kolobov, and Andrey Polezhaev
P. N. Lebedev Physical Institute of the Russian Academy of Sciences, 53 Leninskiy Prospekt, Moscow, Russia
(Received 5 December 2016; published 12 May 2017)

We investigate numerically the behavior of a two-component reaction-diffusion system of Fitzhugh-Nagumo type before the onset of subcritical Turing bifurcation in response to local rigid perturbation. In a large region of parameters, the initial perturbation evolves into a localized structure. In a part of that region, closer to the bifurcation line, this structure turns out to be unstable and covers all the available space over the course of time in a process of self-completion. Depending on the parameter values in two-dimensional (2D) space, this process happens either through generation and evolution of new peaks on oscillatory tails of the initial pattern, or through the elongation, deformation, and rupture of initial structure, leading to space-filling nonbranching snakelike patterns. Transient regimes are also possible. Comparison of these results with 1D simulations shows that the prebifurcation region of parameters where the self-completion process is observed is much larger in the 2D case.

DOI: 10.1103/PhysRevE.95.052208

I. INTRODUCTION

Spatiotemporal patterns formed in systems far from thermodynamic equilibrium are widely spread in nature. They are observed in systems of a different nature: physical, chemical, or biological [1–3]. They often demonstrate an apparent likeness, which implies that their formation is due to some general principles independent of specific details. In view of the similarity of these structures, one may expect that mechanisms revealed for a specific system may be principally the same for systems of various origin. Hence the results obtained experimentally for model chemical systems are of vast importance. Two famous classes of chemical reactions exhibiting rich dynamical behavior are the CIMA (chlorite-iodide-malonic acid) reaction [4] and the BZ (Belousov-Zhabotinsky) reaction [5]. Depending on the concentrations of source reagents, these reactions carried out in a test tube demonstrate a lot of different oscillatory modes, while in a thin flat layer concentration waves are observed. Under sophisticated experimental conditions, these reactions exhibit a variety of complex spatiotemporal patterns. In the CIMA reaction held in a gel—in order to slow down the diffusivity of iodide—nonuniform stationary patterns were first obtained experimentally [6]. A very interesting experimental setup of the BZ reaction was suggested by Vanag and colleagues [7], in which the reaction is performed in a water-in-oil aerosol OT microemulsion (the so-called BZ-AOT system) so that some species can diffuse throughout all the given volume, while others are constrained only to water droplets that collide and exchange their contents. These conditions make it possible to observe a great variety of patterns new to chemical reactions, such as antispirals, wave packets, standing waves, segmented and dotted waves, as well as oscillating clusters and localized oscillating spots—oscillons [8].

These fascinating experimental findings stimulated a vast theoretical investigation of the mechanisms that are responsible for pattern formation [9–14]. It is common knowledge that the formation of stationary nonuniform patterns, i.e., dissipative structures, in reaction-diffusion systems is a consequence of Turing instability, which was theoretically predicted by Turing in his classical paper [15]. Another type of diffusion instability—wave instability—was shown to be responsible for the formation of standing waves, wave packets [16,17], as well as more intricate structures such as antispirals [9,10].

In experiments, two major types of spatially nonuniform structures are observed: nonlocalized patterns that occupy the whole available space, and localized structures that do not spread far away from their place of origin. While in the region of Turing instability nonlocalized dissipative structures are always formed, localized structures can arise in the prebifurcation region of subcritical Turing instability due to large enough initial local excitation [18,19]. Under appropriate parameter values, these structures may evolve into nonlocalized ones due to perturbations. This phenomenon, referred to as self-completion, is considered to be quite general and has been observed in systems of a different nature [20–22]. It has been intensively studied theoretically [23,24] and experimentally [25], including the chemical BZ-AOT system mentioned above [26].

In the present paper, we investigate numerically the self-completion of localized structures in the system of equations of the well-known Fitzhugh-Nagumo type in one- and two-dimensional cases [27]. We show that the region of parameters under which self-completion may take place depends crucially on the dimension of the system, and in the two-dimensional case we demonstrate two qualitatively different types of self-completion mechanism, one of which, to the best of our knowledge, has not been demonstrated in a Fitzhugh-Nagumo-like system before the onset of subcritical Turing bifurcation. Then we examine the dependence of the self-completion type and thereafter of the qualitative appearance of arisen patterns on the parameter values, demonstrating the transition dynamics of the system.

The original Fitzhugh-Nagumo model was suggested as a mathematical simplification of the physiologically based Hodgkin-Huxley model [28]. The Fitzhugh-Nagumo model neglected its biological details, but preserved its essential

*kuznetsovmb@mail.ru

ability to describe the initiation and propagation of action potentials in neurons. The model has also turned out to be very useful for the study of general features of spatiotemporal pattern formation, as it is able to exhibit the majority of pattern types observed in other reaction-diffusion systems [19].

In this paper, we first briefly present a linear analysis of the model to obtain the conditions for Turing instability, then we deduce the amplitude equation for the critical mode, which determines the parametric region of subcritical bifurcation. Finally, we present the results of numeric simulations and discuss them.

II. THE MODEL

We consider the following set of equations:

$$\dot{u} = D\Delta u - u(u+\alpha)(u-1) - v,$$
$$\dot{v} = \Delta v + u - v. \tag{1}$$

There are two control parameters—the ratio of species diffusion coefficients D and the reaction parameter α. D is assumed to be less than unity in order for the activator u to propagate slower than the inhibitor v. The nondistributed system has three pairs of roots: $u = v = 0$ and $u = v = \frac{1}{2}(1 - \alpha \pm \sqrt{\alpha^2 + 2\alpha - 3})$, so the system has only one stationary state $(0;0)$ when $-3 < \alpha < 1$, which is true for all the cases considered herein. This state is stable if for the equations linearized near it the trace of the Jacobian, which is $\alpha - 1$, is negative while its determinant is positive. Both conditions are satisfied since we take $\alpha < 1$. In the distributed system, the trivial homogeneous solution remains stable before the onset of diffusion-driven Turing instability, resulting in the spontaneous formation of stationary nonuniform patterns. Turing bifurcation leads to the instability of waves with wave numbers k for which the roots of the following dispersion equation $\lambda_{1,2}$ are real numbers with opposite signs [29]:

$$\begin{vmatrix} \alpha - k^2 D - \lambda & -1 \\ 1 & -1 - k^2 - \lambda \end{vmatrix} = 0.$$

For all the other waves, both roots $\lambda_{1,2}$ are to be negative since it is assumed that the trace of the system Jacobian, which is the sum of these roots, is negative for $k = 0$ and with increasing k it can only decrease. At the edges of the range of unstable waves, one of the roots turns to zero, so, as follows from the dispersion equation, the waves with wave numbers between k_1 and k_2 are unstable, where

$$k_{1,2}^2 = \frac{\alpha - D \pm \sqrt{(\alpha + D)^2 - 4D}}{2D}.$$

Turing bifurcation takes place when these wave numbers coincide, which means that the radicand of this expression equals zero, while the whole expression is positive. Having already set that $D < 1$, we obtain the final condition for the Turing instability: $1 > \alpha > 2\sqrt{D} - D$, $\alpha_{\text{crit}} = 2\sqrt{D} - D$ is the critical value of the control parameter at which the bifurcation takes place for a given value of D, and $k_{\text{crit}} = \sqrt{\frac{\sqrt{D}-D}{D}}$ is the critical wave number, i.e., the wave number of the wave that becomes unstable first.

To establish the parametric region of interest where the simulations should be performed, we need to determine where the Turing bifurcation is of subcritical type. It implies that just after the onset of the bifurcation, finite-amplitude dissipative structures are formed, while just before it dissipative structures may appear under certain conditions while the trivial stable solution also exists. To find this region, we construct the amplitude equation for the critical mode near the bifurcation. A detailed derivation of this equation is described in Appendix A. As a result, we obtain that when D is less than a certain value, which is approximately equal to 0.094, the system undergoes a subcritical bifurcation, otherwise it undergoes a supercritical one.

III. RESULTS

We performed numerical simulations in a square domain with the side length $L = 20$ in two dimensions and in a segment of the same length in one dimension, setting no-flux boundary conditions using the C++ implemented code. Splitting with respect to physical processes was used. Kinetic equations were solved using the Runge-Kutta fourth-order method. In the 2D case, diffusion equations were solved using the alternating direction implicit method, each one-dimensional problem being solved using the flux sweeping method, which allows for substantially more accurate computations in high gradient regions than ordinary methods do while using the same time and space steps, which is crucial under small values of the parameter D. This method is described in detail in Appendix B. The initial conditions for variables at the moment $t = 0$ were set as

$$u(x,y) = 2v(x,y) = \{1 + 6.25[(x - L/2)^2 + (y - L/2)^2]\}^{-1},$$

thus the initial rigid local perturbation of sufficient magnitude was modeled. Time and space steps were chosen based on the system's kinetic parameters and characteristic wavelengths, and they were set to be $\tau = 5\times10^{-3}$ and $h = 5\times10^{-2}$, respectively. Numerical runs with smaller steps demonstrated no significant difference.

The left graph of Fig. 1 shows the dependence of the type of model response to rigid perturbation on the system parameters in the region before the onset of Turing instability in the two-dimensional case. The parameter of precriticality $\Delta\alpha = \alpha_{\text{crit}} - \alpha$ indicates how far from the bifurcation the system is under a predefined D. To the left of the y-axis there is a region of Turing instability where stationary patterns form spontaneously due to infinitesimal perturbations. It cannot happen in the main graph region, which was systematically checked in numerical simulations. Minus signs indicate the parameter values for which the initial perturbation eventually dies out, while other markers denote the formation of localized structures. For the parameter values indicated by plus signs, these structures over the course of time turn out to be unstable under minor perturbations and evolve, covering all the available space domain. Analogous results for the one-dimensional case are shown in the right graph. The presented results point out that in the 2D case the region where the formation of localized structures may happen is wider than the corresponding region in one dimension. The same is true for the region where self-completion takes place—this

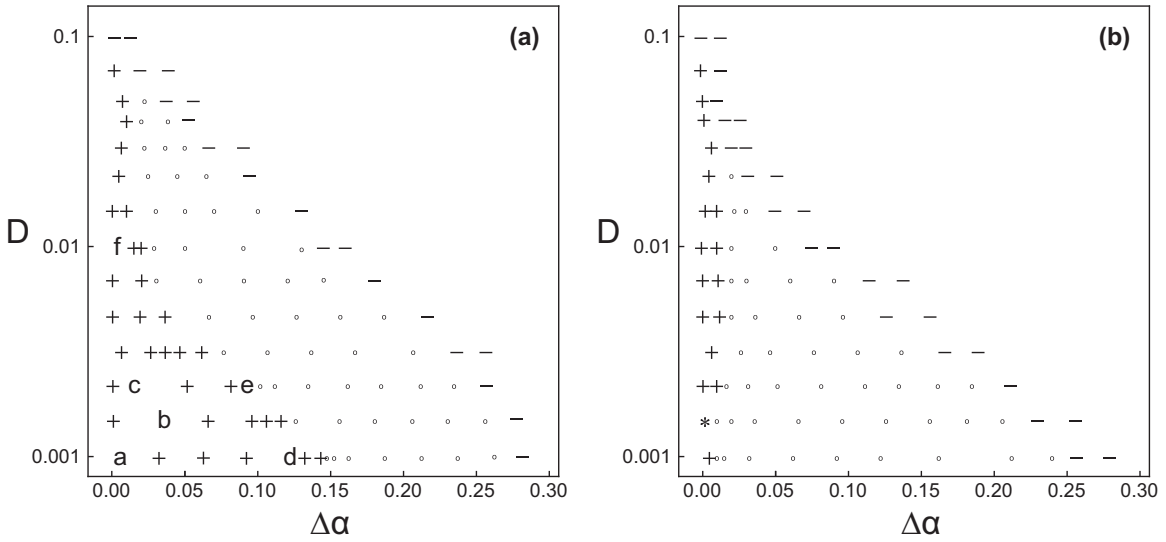

FIG. 1. Type of response of the model, described by Eqs. (1), to initial rigid perturbation depending on the model parameters: (a) in two dimensions, (b) in one dimension. Minus signs indicate initial perturbation extinction over the course of time, dots indicate the formation of stable localized structures, and plus signs indicate the formation of localized structures that evolve into nonlocalized patterns. The dynamics of the one-dimensional self-completion case designated by an asterisk is shown in Fig. 2. The dynamics of the two-dimensional self-completion cases designated by the letters a–f is shown in Fig. 3.

region widens upon increasing the space dimension, especially pronounced at small values of D.

Localized structures arising both in the 1D and 2D cases have the form of axisymmetric large-amplitude peaks with small-amplitude oscillatory tails. Their amplitude decreases and their period increases with growth of D and $\Delta\alpha$. At small values of D and large precriticality, oscillations are overdamped. The dynamics of the one-dimensional self-completion case, marked by an asterisk in Fig. 1, is shown in Fig. 2. In one dimension, all the observed self-completion

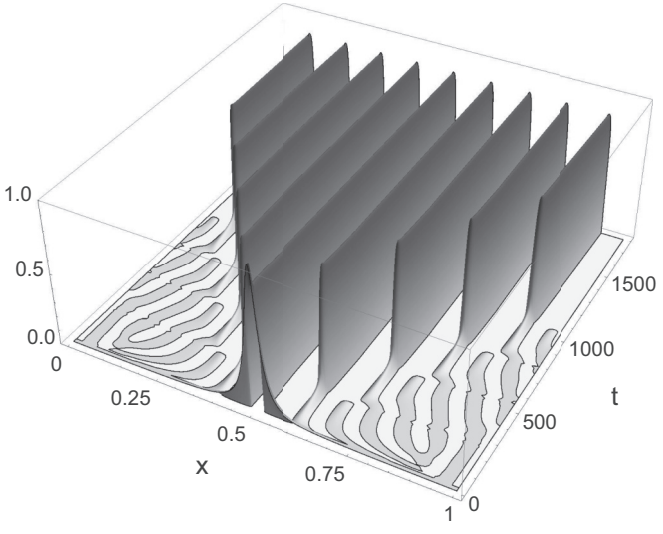

FIG. 2. Self-completion of localized spotlike structures arising in the model, described by Eqs. (1), in the one-dimensional case. Variable u is shown, with white corresponding to negative values, black to maximal positive values, and gray to small positive values. Parameter values are $D = 0.0015$, $\alpha \approx 0.074$, and $\Delta\alpha = 0.002$.

cases occur through the generation of new structures on peaks of oscillatory tails of the initial structure.

Figure 3 demonstrates the dynamics of self-completion in the two-dimensional case for specific values of parameters, which are marked by letters in Fig. 1. In all these and most of the other runs, the initial pattern lost its stability without the intentional addition of noise but due to unavoidable numerical inaccuracies of computations. The system's response to rigid perturbation does not change qualitatively when crossing the line of Turing bifurcation: close to this line in the region of instability, similar structures arise in the same manner as before the onset of bifurcation. As seen from Fig. 3(a), new spots arise around the initial localized structure as a result of rotational symmetry breaking of the oscillatory ring-shaped tails, which are marked in gray. The shape of the newly arisen structures is immediately affected by their neighbors, and new maxima appear in their turn on their oscillatory tails. They build up to new localized deformed spots, with the whole process resulting in a dissipative structure covering all the available space.

When moving away from the bifurcation line at small values of D, another type of self-completion takes place—the initial spot deforms and starts elongating in one direction, corresponding to the one having an increased ratio of activator to inhibitor due to accidental or intentional perturbation. The growing structure folds and corrugates, but never branches, densely occupying all the available space over the course of time. The first elongating patterns that appear with the increase of $\Delta\alpha$ accidentally rupture during their development, but further from the bifurcation line they become more rigid, though they may still rupture at points of high curvature arising due to boundary conditions. An example of this type of growth is a flowerlike pattern, shown in Fig. 3(b), which forms when the line bends in such a way that its ends have no space to grow further and instead its "fingertips" begin to spread away, each of them in its turn splitting into two daughter

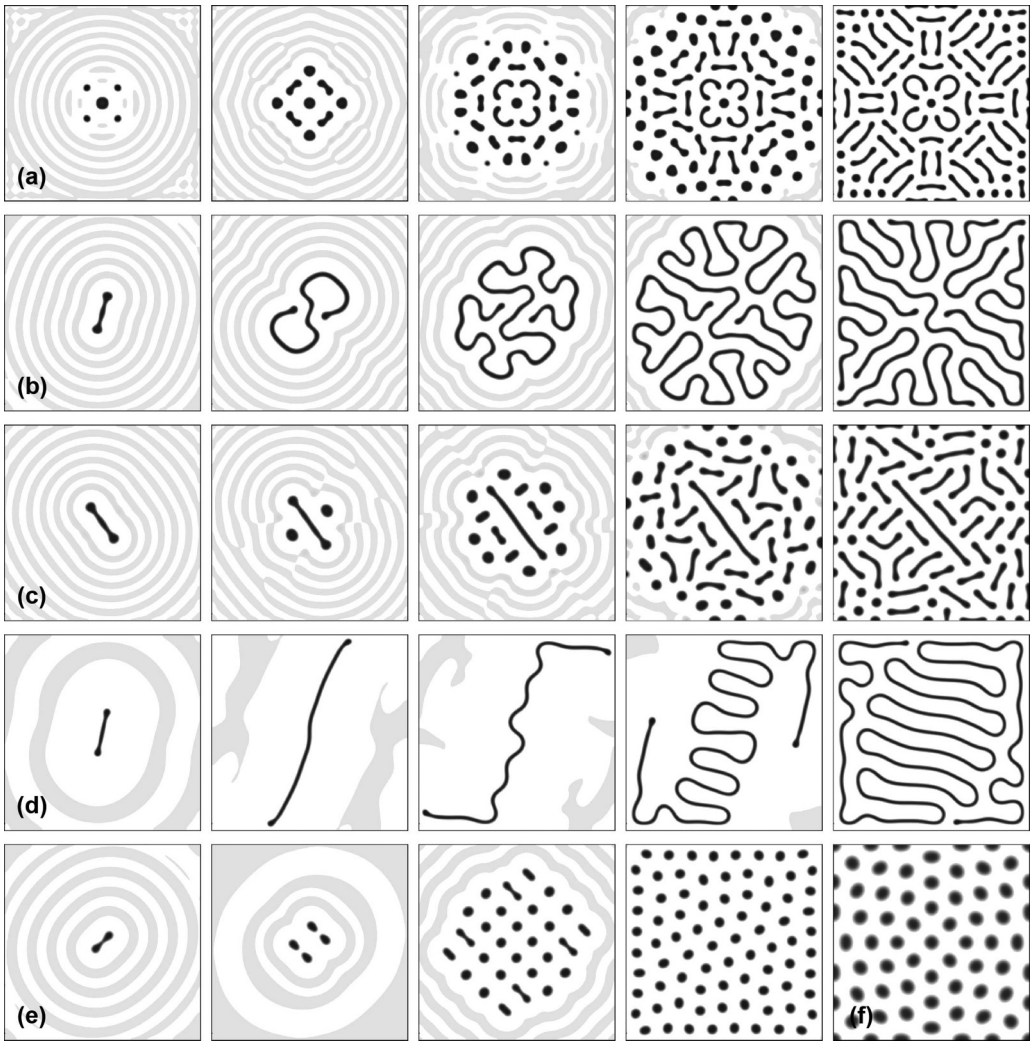

FIG. 3. Self-completion of localized spotlike structures arising in the model (1) in the two-dimensional case. Cases (a)–(e) demonstrate system dynamics under different parameters values, and they comprise five figures in a row each, except for (e), which comprises four figures. Case (f) shows static distribution for one specific case. Variable u is shown, with white corresponding to negative values, black to maximal positive values, and gray to small positive values. Parameters and time values (from left to right) are as follows: (a) $D = 0.001$, $\alpha = 0.057$ ($\Delta\alpha \approx 0.005$); $t = 700$, 1100, 1600, 2200, and 24 000. (b) $D = 0.0015$, $\alpha = 0.04$ ($\Delta\alpha \approx 0.036$); $t = 4800$, 7300, 10 500, 14 000, and 30 000. (c) $D = 0.0022$, $\alpha = 0.077$ ($\Delta\alpha \approx 0.015$); $t = 4300$, 4600, 5100, 6000, and 25 500. (d) $D = 0.001$, $\alpha = -0.06$ ($\Delta\alpha \approx 0.122$); $t = 12\,000$, 18 000, 23 000, 30 500, and 60 000. (e) $D = 0.0022$, $\alpha = 0$ ($\Delta\alpha \approx 0.092$); $t = 42\,800$, 44 800, 55 000, and 84 500. (f) $D = 0.01$, $\alpha = 0.185$ ($\Delta\alpha \approx 0.005$); $t = 3000$. $\Delta\alpha = 2\sqrt{D} - D - \alpha$.

tips. There also exist transitive situations when both types of self-completion—by arising new localized structures and by deformation—coexist, as shown in Fig. 3(c).

With the decrease of the control parameter α and thus moving away from the bifurcation line, the rate of the self-completion process decreases and its behavior changes qualitatively. The nature of this change differs for different values of D. When D is less than $\approx$0.002, with the growth of $\Delta\alpha$ the rigidity of the line structures continues to grow, as demonstrated in Fig. 3(d), until the region in parametric space is reached where self-completion ceases and initially arisen structures remain localized. However, for larger values of D with the increase of $\Delta\alpha$ the line structures rupture more frequently, and quite near the edge of the self-completion region they begin to break apart pretty soon after initial deformation into spotlike structures, which then elongate into the perpendicular direction. This process repeats, resulting in a dot-covered domain shown in Fig. 3(e). A similar resulting pattern, like the one demonstrated in Fig. 3(f), is obtained near the bifurcation line for larger values of D—closer to the transition from sub- to supercritical type of bifurcation—but the dynamics leading to this pattern is completely different as these structures arise on oscillatory tails of already existing ones in the above-described manner.

IV. DISCUSSION

Fitzhugh-Nagumo-like reaction-diffusion models are of great importance, as they are able to exhibit a large number of pattern formation phenomena, which are listed, e.g., in [19]. In this paper, we present our systematic study of the behavior of the corresponding system in a sufficiently

wide parametric range before the onset of subcritical Turing bifurcation. In a large region, localized stationary structures arise in response to strong enough initial local excitation. Close to the bifurcation line due to small perturbations, they evolve into nonlocalized dissipative structures in a process referred to as self-completion. We demonstrate two qualitatively different types of self-completion mechanism in the two-dimensional case. One of them, which has already been shown for Fitzhugh-Nagumo-like models, happens via the appearance and evolution of new localized structures on the oscillatory tail of the initial one. The other one, which, to the best of our knowledge, has not been demonstrated in a Fitzhugh-Nagumo-like system before the onset of subcritical Turing bifurcation, is the development of a snakelike pattern through elongation, deformation, and rupture of the initial localized structure. The objective difficulty hindering this investigation is that in the considered parametric region—namely, when the diffusion coefficients differ up to several orders of magnitude—one has to deal with extremely stiff equations, which pose essential problems for simulations. We have overcome this difficulty by using an efficient numerical scheme based on the method that is, to the best of our knowledge, not used in standard PDE solvers, and therefore the scheme is described briefly in Appendix B.

A similar investigation of parameter space preceding subcritical Turing bifurcation has been carried out for other systems, and through comparing these studies, essential differences in the behavior of basic models can be revealed. For instance, in the two-variable Oregonator model [26], the initial spotlike structure can lose its stability by producing new spots and by splitting into two spots as well, but also by emitting a circular wave, which was not found for the Fitzhugh-Nagumo-like system considered herein. On the other hand, a loss of stability through elongation of a structure and the formation of snakelike space-filling patterns were not reported for that case.

A similar type of self-completion was already observed in a model of Fitzhugh-Nagumo type but in a bistable regime as a result of a competition between regions of two stable states. That phenomenon was thoroughly studied both theoretically [30,31] and experimentally [32]. The model derived to describe the experimental results considered interaction between activation, related to the curvature of the boundary, and long-distance inhibition via coupling of interface segments [33], which resulted in a Fitzhugh-Nagumo equation form. However, as the mechanism governing that process is different, there is a considerable qualitative distinction in developed structures in these two cases—the model investigated herein produces only nonbranching curves under considered parameter values, while at points of high curvature the structures obtained at the bistable regime branch out instead of rupturing.

Another investigation related to the topic is the study of the Gray-Scott model [34], which possesses saddle-node, Turing, and Hopf instabilities, their interaction giving rise to a striking variety of spatiotemporal patterns. For the widely considered relation of variable diffusivities, equal to 2, in the region where pure Turing modes exist, its bifurcation is subcritical [35] and the system is also able to produce snakelike structures, however they are also qualitatively different from the ones reported herein, e.g., they are not able to elongate via "fingertips" when their ends run into an obstacle. The evolution of localized spots to space-filling curves in the parameter region preceding subcritical Turing bifurcation was claimed to be found elsewhere as well [20,36], which infers universality of this type of self-completion. It should also be mentioned, though it is not surprising, that a similar process may also take place in systems that are already in the Turing instability region [37,38].

Numerical simulations for one- and two-dimensional spatial cases detected an essential difference between them in the behavior of the Fitzhugh-Nagumo-like model. For the 2D case, the parametric domain within which nonlocalized patterns are formed is significantly larger, and a qualitative type of self-completion depends on the values of the parameters. In the region of parameter space where in the 2D case self-completion of initial localized structures happens through elongation mechanism, in the 1D case localized structures remain stable. The reason for this striking difference is apparently due to the break of cylindrical symmetry of the initial circular spot, which is impossible in one dimension. This effect resembles a loss of stability of a localized propagating structure with increasing dimension due to transverse instability [39], and it requires further investigation.

ACKNOWLEDGMENT

The authors are thankful for partial support from RFBR Grant No. 17-01-00070 and to the anonymous referees for their constructive comments on the manuscript.

APPENDIX A: AMPLITUDE EQUATION FOR THE CRITICAL MODE

The purpose of the derivation of the amplitude equation herein is to reveal the region in which Turing bifurcation is of subcritical type. There are several approaches to derive amplitude equations. The one that we use is based on a multiscale technique described, for instance, in [40].

Let us represent Eqs. (1) in the following form:

$$\frac{\partial \mathbf{x}}{\partial t} = \mathscr{L}_0(\alpha)\mathbf{x} + \mathscr{L}_1(D)\Delta\mathbf{x} + \mathbf{h}(\mathbf{x},\alpha),$$

where $\mathbf{x} = \binom{u}{v}$, $\mathscr{L}_0(\alpha) = \begin{pmatrix}\alpha & -1\\ 1 & -1\end{pmatrix}$, $\mathscr{L}_1(D) = \begin{pmatrix}D & 0\\ 0 & 1\end{pmatrix}$, and $\mathbf{h}(\mathbf{x},\alpha) = \binom{-u^3 + (1-\alpha)u^2}{0}$.

The value of the critical parameter under which Turing bifurcation takes place is $\alpha_{\rm cr} = 2\sqrt{D} - D$, the square of the critical wavelength being $k_{\rm cr}^2 = \frac{\sqrt{D}-D}{D}$.

The decomposition of variables with respect to auxiliary smallness parameter ϵ has the following form:

$$\begin{aligned} \mathbf{x} &= \epsilon\mathbf{x_1} + \epsilon^2\mathbf{x_2} + \epsilon^3\mathbf{x_3} + \cdots,\\ \alpha - \alpha_{\rm cr} &= \epsilon^2\gamma_2 + \cdots,\\ \frac{\partial}{\partial t} &= \epsilon^2\frac{\partial}{\partial \tau} + \cdots. \end{aligned} \tag{A1}$$

Linear terms in decompositions of $\alpha - \alpha_{\rm cr}$ and $\frac{\partial}{\partial t}$ are known to be equal to zero for the considered type of instability, thus reflecting the spatial symmetries of the system. We consider the system of small spatial extent, so in some vicinity to the

bifurcation line only one mode is destabilized, therefore no additional scaling of space derivatives is needed.

To the first order of ϵ, considering the one-dimensional case for simplicity, we get the set of equations

$$\left[\mathscr{L}_0(\alpha_{\rm cr})+\mathscr{L}_1(D)\frac{\partial^2}{\partial r^2}\right]\mathbf{x_1}=0.$$

We seek a solution in the form

$$\mathbf{x_1}=c(\tau)\mathbf{u}e^{ik_{\rm cr}r}+cc,$$

where $c(\tau)$ is the amplitude of the solution. It gives

$$\begin{pmatrix}\alpha_{\rm cr}-Dk_{\rm cr}^2 & -1\\ 1 & -1-k_{\rm cr}^2\end{pmatrix}\begin{pmatrix}u_1\\ v_1\end{pmatrix}=0.$$

Let us choose

$$\begin{pmatrix}u_1\\ v_1\end{pmatrix}=\begin{pmatrix}1\\ \alpha_{\rm cr}-Dk_{\rm cr}^2\end{pmatrix}=\begin{pmatrix}1\\ \sqrt{D}\end{pmatrix}.$$

Then

$$\mathbf{x_1}=c\begin{pmatrix}1\\ \sqrt{D}\end{pmatrix}e^{ik_{\rm cr}r}+c^*\begin{pmatrix}1\\ \sqrt{D}\end{pmatrix}e^{-ik_{\rm cr}r}.$$

To the second order of ϵ, we obtain

$$\left[\mathscr{L}_0(\alpha_{\rm cr})+\mathscr{L}_1(D)\frac{\partial^2}{\partial r^2}\right]\mathbf{x_2}=-\frac{1}{2}\mathbf{h_{xx}}(\alpha_{\rm cr})\mathbf{x_1}\mathbf{x_1},$$

or

$$\begin{pmatrix}\alpha_{\rm cr}+D\frac{\partial^2}{\partial r^2} & -1\\ 1 & -1+\frac{\partial^2}{\partial r^2}\end{pmatrix}\mathbf{x_2}=-\begin{pmatrix}(1-\alpha_{\rm cr})[\{c^2e^{2ik_{\rm cr}r}+cc\}+2|c|^2]\\ 0\end{pmatrix}.$$

We seek a solution in the form $\mathbf{x_2}=(\frac{u_2}{v_2})=(\frac{p_0}{q_0})|c|^2+[(\frac{p_1}{q_1})c^2e^{2ik_{\rm cr}r}+cc]$. It gives $p_0=q_0=2$, $p_1=\frac{4\sqrt{D}-3D}{9D}$, and $q_1=\frac{1}{9}$.

To the third order of ϵ, we get

$$\left[\mathscr{L}_0(\alpha_{\rm cr})+\mathscr{L}_1(D)\frac{\partial^2}{\partial r^2}\right]\mathbf{x_3}=-\gamma_2\mathscr{L}_{0\alpha}(\alpha_{\rm cr})\mathbf{x_1}-\mathbf{h_{xx}}(\alpha_{\rm cr})\mathbf{x_1}\mathbf{x_2}-\frac{1}{6}\mathbf{h_{xxx}}(\alpha_{\rm cr})\mathbf{x_1}\mathbf{x_1}\mathbf{x_1}+\frac{\partial\mathbf{x_1}}{\partial\tau}=\mathbf{q_3}.$$

The solvability condition is

$$\int_0^{\frac{2\pi}{k_{\rm cr}}}dr\,\mathbf{u}^{+*}\cdot\mathbf{q_3}(c,\tau,r)=0,$$

where $\mathbf{u}^{+*}$ is the eigenvector of $\mathscr{L}^+(\alpha_{\rm cr},D)=\mathscr{L}_0^+(\alpha_{\rm cr})+\mathscr{L}_1^+(D)\frac{\partial^2}{\partial r^2}$, which is up to a factor equal to $(\frac{-1}{\sqrt{D}})e^{-ik_{\rm cr}r}$.

When integrating, a nonzero contribution is given only by terms $\mathbf{q_3}$, containing the factor $e^{ik_{\rm cr}r}$. They are

$$\left[-\gamma_2\begin{pmatrix}1&0\\0&0\end{pmatrix}\begin{pmatrix}1\\ \sqrt{D}\end{pmatrix}c-\begin{pmatrix}(1-\alpha_{\rm cr})[4+\frac{8\sqrt{D}-6D}{9D}]-3\\ 0\end{pmatrix}|c|^2c+\frac{\partial c}{\partial\tau}\begin{pmatrix}1\\ \sqrt{D}\end{pmatrix}\right]e^{ik_{\rm cr}r}.$$

As a result of calculations, replacing $z=\epsilon c$, we obtain an equation of the form

$$\frac{\partial z}{\partial t}=(\alpha-\alpha_{\rm cr})P_1z+P_3|z|^2z,$$

where $P_1=\dfrac{1}{1-D}$,

$$P_3=\frac{30D^2-52D\sqrt{D}-13D+8\sqrt{D}}{9D(1-D)}.$$

Since we consider $0<D<1$, P_1 is positive and the sign of P_3 determines the type of bifurcation. It changes at $D=D_c\approx 0.094$—when D is less than this value, the system undergoes a subcritical bifurcation, otherwise it undergoes a supercritical one. This result is the same for any space dimensions as it is not affected by the interplay of modes.

APPENDIX B: FLUX SWEEPING METHOD

Numerically solving diffusion equations results in certain difficulties when dealing with high gradients of variables. To avoid these difficulties and to speed up the computations, we switch from second-order equations to a system of first-order equations by implementing the flux sweeping method in the following way, which is based on a method described in [41].

First, we represent each of the diffusion equations as follows:

$$\frac{\partial u}{\partial t}=\frac{\partial P}{\partial x},\quad P=D\frac{\partial u}{\partial x},$$

and we write down the difference equations:

$$\frac{u_m^{n+1}-u_m^n}{\tau}=\frac{Q_{m+1/2}-Q_{m-1/2}}{h},\quad m=0,1,\ldots,N,$$

$$Q_{m+1/2}=D\frac{u_{m+1}^{n+1}-u_m^{n+1}}{h},\quad m=0,1,\ldots,N-1,$$

where τ and h are time and space steps, and indices n and m represent numbers of time and space steps, respectively. The sweeping relation has the form

$$u_m^{n+1}=P_mQ_{m+1/2}+R_m,$$

where sweeping coefficients P_m and R_m are to be determined. We use zero-flux boundary conditions, so we take $Q_{-1/2}$ to be equal to $-Q_{1/2}$. Therefore, we set the zeroth coefficients to be $P_0=\frac{2\tau}{h}$, $R_0=u_0^n$. To obtain the formulas for subsequent coefficients for $m=1,2,\ldots,N$, we substitute the already known sweeping relation for u_{m-1}^{n+1} into the expression for $Q_{m+1/2}$ and get

$$u_m^{n+1}=\left(P_{m-1}+\frac{h}{D}\right)Q_{m-1/2}+R_{m-1},$$

from which using the first difference equation we replace $Q_{m-1/2}$ obtaining the linear dependence of u_m^{n+1} by $Q_{m+1/2}$, thus finding the following coefficients:

$$P_m=\left[P_{m-1}+\frac{h}{D}\right]\Big/\left(1+\frac{h}{\tau}\left[P_{m-1}+\frac{h}{D}\right]\right),$$

$$R_m=\left(R_{m-1}+\frac{h}{\tau}\left[P_{m-1}+\frac{h}{D}\right]u_m^n\right)\Big/\left(1+\frac{h}{\tau}\left[P_{m-1}+\frac{h}{D}\right]\right).$$

At the right border, we use the same zero-flux boundary condition, so we state using the first difference equation that $Q_{N+1/2} = -Q_{N-1/2} = \frac{h}{2\tau}(u_N^{n+1} - u_N^n)$, and we substitute it into the sweeping relation for u_N^{n+1}, finding the following value:

$$u_N^{n+1} = \left(R_N - \frac{h}{2\tau} P_N u_N^n\right) \Big/ \left(1 - \frac{h}{2\tau} P_N\right).$$

Then we find the complete variable array at the time step $n+1$ by expressing

$$Q_{m+1/2} = Q_{m+3/2} - \frac{h}{\tau}\left(u_{m+1}^{n+1} - u_{m+1}^n\right),$$

$$u_m^{n+1} = P_m Q_{m+1/2} + R_m$$

for $m = N-1,\ N-2, \ldots, 0$.

[1] J. P. Gollub and J. Langer, Rev. Mod. Phys. **71**, S396 (1999).
[2] M. Wu, G. Ahlers, and D. S. Cannell, Phys. Rev. Lett. **75**, 1743 (1995).
[3] E. Ben-Jacob, I. Cohen, and H. Levine, Adv. Phys. **49**, 395 (2000).
[4] P. De Kepper, I. R. Epstein, K. Kustin, and M. Orban, J. Phys. Chem. **86**, 170 (1982).
[5] J. Lindsay, R. J. Field, and M. Burger, *Oscillations and Traveling Waves in Chemical Systems* (Wiley, New York, 1985).
[6] V. Castets, E. Dulos, J. Boissonade, and P. De Kepper, Phys. Rev. Lett. **64**, 2953 (1990).
[7] V. K. Vanag, Usp. Fiz. Nauk **174**, 991 (2004).
[8] V. K. Vanag and I. R. Epstein, in *Self-Organized Morphology in Nanostructured Materials* (Springer, Berlin, 2008), pp. 89–113.
[9] Y. Gong and D. J. Christini, Phys. Rev. Lett. **90**, 088302 (2003).
[10] V. K. Vanag and I. R. Epstein, Science **294**, 835 (2001).
[11] V. K. Vanag and I. R. Epstein, Proc. Natl. Acad. Sci. USA **100**, 14635 (2003).
[12] M. Y. Borina and A. Polezhaev, Comput. Res. Model. **5**, 533 (2013) (in Russian).
[13] D. M. Petrich and R. E. Goldstein, Phys. Rev. Lett. **72**, 1120 (1994).
[14] A. Hagberg and E. Meron, Chaos **4**, 477 (1994).
[15] A. M. Turing, Philos. Trans. R. Soc. London, Ser. B **237**, 37 (1952).
[16] M. Dolnik, A. M. Zhabotinsky, A. B. Rovinsky, and I. R. Epstein, Chem. Eng. Sci. **55**, 223 (2000).
[17] A. A. Polezhaev and M. Y. Borina, in *Nonlinear Dynamics of Electronic Systems, Proceedings of NDES 2012* (VDE, Wolfenbüttel, 2012), pp. 1–4.
[18] O. Jensen, V. O. Pannbacker, E. Mosekilde, G. Dewel, and P. Borckmans, Phys. Rev. E **50**, 736 (1994).
[19] H.-G. Purwins, H. Bödeker, and S. Amiranashvili, Adv. Phys. **59**, 485 (2010).
[20] L. Spinelli, G. Tissoni, M. Brambilla, F. Prati, and L. A. Lugiato, Phys. Rev. A **58**, 2542 (1998).
[21] E. Meron, E. Gilad, J. von Hardenberg, M. Shachak, and Y. Zarmi, Chaos Solitons Fractals **19**, 367 (2004).
[22] M. Tlidi, A. G. Vladimirov, and P. Mandel, Phys. Rev. Lett. **89**, 233901 (2002).
[23] Y. Nishiura and D. Ueyama, Physica D **130**, 73 (1999).
[24] W. N. Reynolds, J. E. Pearson, and S. Ponce-Dawson, Phys. Rev. Lett. **72**, 2797 (1994).
[25] Y. A. Astrov and Y. A. Logvin, Phys. Rev. Lett. **79**, 2983 (1997).
[26] A. Kaminaga, V. K. Vanag, and I. R. Epstein, Angew. Chem., Int. Ed. **45**, 3087 (2006).
[27] C. Rocsoreanu, A. Georgescu, and N. Giurgiteanu, *The FitzHugh-Nagumo Model: Bifurcation and Dynamics* (Springer Science & Business Media, Berlin, 2012), Vol. 10.
[28] A. L. Hodgkin and A. F. Huxley, J. Physiol. **117**, 500 (1952).
[29] J. D. Murray, *Mathematical Biology. II. Spatial Models and Biomedical Applications Interdisciplinary Applied Mathematics Vol. 18* (Springer-Verlag, New York, 2001).
[30] R. E. Goldstein, D. J. Muraki, and D. M. Petrich, Phys. Rev. E **53**, 3933 (1996).
[31] C. B. Muratov and V. V. Osipov, Phys. Rev. E **54**, 4860 (1996).
[32] K. J. Lee, W. McCormick, Q. Ouyang, and H. L. Swinney, Science **261**, 192 (1993).
[33] C. B. Muratov, Phys. Rev. E **66**, 066108 (2002).
[34] J. E. Pearson, Science **261**, 189 (1993).
[35] W. Mazin, K. Rasmussen, E. Mosekilde, P. Borckmans, and G. Dewel, Math. Comput. Simul. **40**, 371 (1996).
[36] A. Yochelis, Y. Tintut, L. Demer, and A. Garfinkel, New J. Phys. **10**, 055002 (2008).
[37] P. Davies, P. Blanchedeau, E. Dulos, and P. De Kepper, J. Phys. Chem. A **102**, 8236 (1998).
[38] T. Kolokolnikov and M. Tlidi, Phys. Rev. Lett. **98**, 188303 (2007).
[39] A. Hagberg and E. Meron, Phys. Rev. E **57**, 299 (1998).
[40] G. Nicolis, *Introduction to Nonlinear Science* (Cambridge University Press, Cambridge, 1995).
[41] R. P. Fedorenko, *Introduction to Computational Physics* (MPTI, Moscow, 1994) (in Russian).